

# Selective Modulation of Histaminergic Inputs on Projection Neurons of Cerebellum Rapidly Promotes Motor Coordination via HCN Channels

Jun Zhang · Qian-Xing Zhuang · Bin Li · Guan-Yi Wu ·  
Wing-Ho Yung · Jing-Ning Zhu · Jian-Jun Wang

Received: 15 October 2014 / Accepted: 12 January 2015 / Published online: 30 January 2015  
© Springer Science+Business Media New York 2015

**Abstract** Insights into function of central histaminergic system, a general modulator originating from the hypothalamus for whole brain activity, in motor control are critical for understanding the mechanism underlying somatic-nonsomatic integration. Here, we show a novel selective role of histamine in the cerebellar nuclei, the final integrative center and output of the cerebellum. Histamine depolarizes projection neurons but not interneurons in the cerebellar nuclei via the hyperpolarization-activated cyclic nucleotide-gated (HCN) channels coupled to histamine H2 receptors, which are exclusively expressed on glutamatergic and glycinergic projection neurons. Furthermore, blockage of HCN channels to block endogenous histaminergic afferent inputs in the cerebellar nuclei significantly attenuates motor balance and coordination. Therefore, through directly and quickly modulation on projection neurons but not interneurons in the cerebellar nuclei,

central histaminergic system may act as a critical biasing force to not only promptly regulate ongoing movement but also realize a rapid integration of somatic and nonsomatic response.

**Keywords** Histamine · Histamine H2 receptor · HCN channel · Cerebellar nuclei · Projection neurons · Motor control

## Introduction

A behavioral response needs a coordinated and harmonious integration of somatic movements with nonsomatic activities, such as visceral, emotional, cognitive, and other components [1, 2]. As a general modulator for whole brain activity, the central histaminergic system, originating from the tuberomammillary nucleus of the hypothalamus, not only participates in regulation of various nonsomatic functions but also holds a key position in somatic motor control [1, 3, 4]. In this system, the direct hypothalamocerebellar projections [5], bridging the hypothalamus, a high center for autonomic (nonsomatic) regulation, and the cerebellum, a classic subcortical motor structure, are presumably considered to participate in motor control and be potential pathways underlying the somatic-nonsomatic integration [1, 6]. Intriguingly, the projections extensively exist in both nonmammalian vertebrates and mammals and appear to be stronger in species ascending the phylogenetic scale [6], indicating the connections may not only be phylogenetically old pathways but also play a more important role in brain functions.

The histaminergic hypothalamocerebellar fibers innervating both cortex and nuclei of the cerebellum have been well documented in rat, guinea pig, and human [7–9].

---

Jun Zhang, Qian-Xing Zhuang and Bin Li contributed equally to this work.

**Electronic supplementary material** The online version of this article (doi:10.1007/s12035-015-9096-3) contains supplementary material, which is available to authorized users.

---

J. Zhang · Q.-X. Zhuang · B. Li · G.-Y. Wu · J.-N. Zhu (✉) ·  
J.-J. Wang (✉)

State Key Laboratory of Pharmaceutical Biotechnology and  
Department of Biological Science and Technology, School of Life  
Sciences, Nanjing University, Mailbox 426, 22 Hankou Road,  
Nanjing 210093, China  
e-mail: jnzhu@nju.edu.cn  
e-mail: jjwang@nju.edu.cn

W.-H. Yung  
School of Biomedical Sciences, Faculty of Medicine, The Chinese  
University of Hong Kong, Shatin, Hong Kong, China

J. Zhang  
Department of Physiology, Third Military Medical University,  
Chongqing 400038, China

Autoradiographic mapping, immunohistochemical analysis and *in situ* hybridization data have also indicated the presence of histamine receptors in the cerebellum [10–13]. Interestingly, by using extracellular recordings on rat brain slices, we find that histamine excites cerebellar Purkinje cells, granule cells, and nuclear neurons [1, 14], and improves motor performances mediated by the cerebellar interpositus nucleus (IN) or fastigial nucleus (FN) [14, 15]. However, the precise function and mechanism of histaminergic modulation on the cerebellar neuronal circuitry, particularly the action of histamine on various neuronal components in the cerebellar nuclei, is still little known.

Two different types of neurons, the projection neurons and interneurons, are heterogeneously distributed throughout the cerebellar nuclei [16], the final integrative processing unit of the cerebellum and the only sources of the cerebellofugal projections except the flocculonodular lobe [17–20]. The cerebellar nuclear projection neurons are medium- and large-sized cells (diameters ranging from 15 to 35  $\mu\text{m}$ ) and project long axons out of the cerebellar nuclei, whereas the interneurons have small somata (diameters ranging from 5 to 15  $\mu\text{m}$ ) and their short axons only connect with neurons within the cerebellar nuclei [21–23]. Therefore, in the present study, on the basis of electrophysiological and morphological identifications, the effects of histamine on each type of the neurons in the cerebellar nuclear circuitry and the underlying ionic mechanism were investigated at molecular, cellular and behavioral levels. Intriguingly, the results demonstrate that histamine selectively depolarizes projection neurons but not interneurons in the cerebellar nuclei, and promptly improves cerebellar nuclei-mediated motor balance and coordination via hyperpolarization-activated cyclic nucleotide-gated (HCN) channels coupled to histamine H<sub>2</sub> receptors.

## Materials and Methods

### Animals

Sprague-Dawley rats were individually housed under controlled environmental conditions ( $22\pm 2$  °C,  $60\pm 5$  % humidity, and 12-h light/dark cycle with lights on at 8:00 a.m. daily). The animals had free access to standard laboratory chow and water. All experiments were treated in accordance with the US National Institutes of Health Guide for the Care and Use of Laboratory Animals (NIH Publication 80-23, revised 1996). All efforts were made to minimize the number of animals used and their suffering.

### Whole-Cell Patch Clamp Recordings

Under sodium pentobarbital (40 mg/kg) anesthesia, rats aged 12–18 days of either sex were decapitated, since the

histaminergic fibers reach an adult-like appearance about 2 weeks postnatally [4]. After carefully removing the skull, the brain was quickly transferred and immersed in ice-cold artificial cerebrospinal fluid (ACSF, composition in mM: 124 NaCl, 2.5 KCl, 1.25  $\text{NaH}_2\text{PO}_4$ , 1.3  $\text{MgSO}_4$ , 26  $\text{NaHCO}_3$ , 2  $\text{CaCl}_2$ , and 20 D-glucose) equilibrated with 95 %  $\text{O}_2$  and 5 %  $\text{CO}_2$ . The parasagittal slices (300  $\mu\text{m}$  thick) of the cerebellum were cut with a vibroslicer (VT 1200 S, Leica, Nussloch, Germany). According to the rat brain atlas of Paxinos and Watson [24], the slices containing FN, IN, or dentate nucleus (DN) were identified, chosen, and incubated in oxygenated ACSF at  $35\pm 0.5$  °C for at least 1 h and then maintained at room temperature. During recording sessions, the slices were transferred to a submerged chamber and continuously perfused with oxygenated ACSF at a rate of 2 ml/min maintained at  $32\pm 0.5$  °C.

Whole-cell patch recordings were performed as previous reports [2, 25] on cerebellar nuclear neurons with borosilicate glass pipettes (2.5–6 M $\Omega$ ) filled with an internal solution (composition in mM: 135 K-methylsulfate, 5 KCl, 2  $\text{MgCl}_2$ , 10 HEPES, 5 EGTA, 0.5  $\text{CaCl}_2$ , 4  $\text{Na}_2\text{-ATP}$ , 0.4 GTP-Tris, adjusted to pH 7.25 with 1 M KOH). During recording sessions, cerebellar nuclear projection neurons or interneurons were visualized with an Olympus BX51WI microscope (Tokyo, Japan) equipped with infrared differential interference contrast. All images were captured with a charge-coupled device (CCD) camera (4912-5010, Cohu, Poway, CA) displayed on a television monitor and stored in a laboratory computer. Patch-clamp recordings were acquired with an Axopatch-200B amplifier (Axon Instruments, Sunnyvale, CA) and the signals were fed into the computer through a Digidata-1322A interface (Axon Instruments) for data capture and analysis (pClamp 8.2, Axon Instruments). Recordings of whole-cell currents were lowpass filtered at 2 kHz and digitized at 10 kHz, and recordings of membrane potentials were lowpass filtered at 5 kHz and digitized at 20 kHz. Neurons were held at a membrane potential of  $-60$  mV and characterized by injection of rectangular voltage pulse (5 mV, 50 ms) to monitor the whole-cell membrane capacitance, series resistance, and membrane resistance. Neurons were excluded from the study if the series resistance was not stable or exceeded 20 M $\Omega$ .

We bathed the slices with histamine (10–100  $\mu\text{M}$ , Sigma, St. Louis, MO) to stimulate the recorded cerebellar nuclear neurons. Before bath application of histaminergic compounds at known concentrations, the whole-cell current of the recorded neuron was observed for at least 20 min to assure stability. Then, histamine was added to the perfusing ACSF to stimulate the recorded neuron for a test period of 1 min. After each stimulation, cells were given at least 20 min for recovery and prevention of desensitization. TTX (0.3  $\mu\text{M}$ , Alomone Labs, Jerusalem, Israel) was used to determine whether the effect of histamine is postsynaptic. Selective antagonists for histamine H<sub>1</sub>, H<sub>2</sub>, and H<sub>4</sub> receptors, triprolidine (3  $\mu\text{M}$ ,

Tocris, Bristol, UK), ranitidine (3  $\mu$ M, Tocris), and JNJ777120 (3  $\mu$ M, a generous gift from Dr. Rob Leurs, VU University Amsterdam, The Netherlands) were applied to examine the underlying postsynaptic receptor mechanism. Furthermore, to assess the ionic mechanism and characteristic of histamine-induced whole cell current, current-voltage plots ( $I$ - $V$  curves) were obtained before and during histamine application using a step current injection (ranging from  $-90$  to  $-200$  pA in 10 pA steps) in current-clamp recording [2, 25]. In addition, to examine the effect of histamine on HCN channel current,  $I$ - $V$  curves were obtained before and during histamine application using a series of 1 s hyperpolarizing voltage steps (ranging from  $-50$  to  $-120$  mV in 10 mV steps) in voltage-clamp recording [26]. ZD7288 (50  $\mu$ M, Tocris) was applied to block HCN channels. The antagonists/blockers were given for at least 15 min before we observed their antagonistic/blocking effects.

#### Immunofluorescence and Laser Confocal Imaging

The experimental procedures for immunostaining followed our previous reports [2, 25]. Rats (weighing 150–200 g) were deeply anesthetized with sodium pentobarbital and perfused transcardially with 100 ml normal saline, followed by 250–300 ml 4 % paraformaldehyde in 0.1 M phosphate buffer. Subsequently, the brain was removed, trimmed, and postfixed in the same fixative for 12 h at 4 °C, and then cryoprotected with 30 % sucrose for 48 h. Frozen coronal sections (25  $\mu$ m thick) containing cerebellar nuclei were obtained by using a freezing microtome (CM3050S, Leica) and mounted on gelatin-coated slides. The slices were rinsed with PBS containing 0.1 % Triton X-100 and then incubated in 10 % normal bovine serum in PBS containing 0.1 % Triton X-100 for 30 min. Sections were incubated overnight at 4 °C with primary antibodies: rabbit anti-H1 receptor polyclonal antibody (1:50, Santa Cruz Biotech, Dallas, TX), rabbit anti-H2 receptor polyclonal antibody (1:50, Santa Cruz Biotech), rabbit anti-H4 receptor polyclonal antibody (1:50, Santa Cruz Biotech), goat anti-H2 receptor polyclonal antibody (1:200, Everest Biotech, Oxfordshire, UK), goat anti-VGLUT2 (1:300, Abcam, Cambridge, MA), sheep anti-GLYT2 (1:50, Alpha Diagnostic International, San Antonio, TX), mouse anti-GAD67 (1:500, EMD Millipore Corporation, Billerica, MA). After a complete wash in PBS, the sections for single, double, and triple immunostaining were incubated in the related Alexa 488-, Alexa 594-, and/or Alexa 350-conjugated secondary antibodies (1:2,000; Invitrogen, Carlsbad, CA) for 2 h at room temperature in the dark. The slides were washed and mounted in Fluoromount-G mounting medium (SouthernBiotech, Birmingham, AL). Incubations replacing the primary antiserum with control immunoglobulins and/or omitting the primary antiserum were used as negative controls. All micrographs were taken with an inverted laser

scanning confocal FluoView FV1000 microscope (Olympus), equipped with Plan-Apochromat  $\times 60/1.42$  NA oil,  $\times 40/0.9$  NA dry,  $\times 20/0.75$  NA dry, and  $\times 10/0.4$  NA dry objective lenses. Digital images from the microscope were recorded with FV10-ASW 3.1 Viewer Software (Olympus) and image processing was done with Photoshop (Adobe).

#### Single-Cell RT-PCR

Borosilicate glass pipette was pulled and filled with 3.5  $\mu$ l of RNase-free internal solution. Under visual inspection and electrophysiological identification, cerebellar nuclear projection neuron or interneuron was patched, and cytoplasm of the neuron was harvested into pipette with negative pressure. Then, by applying positive pressure, the pipette contents were released into an RNase-free microcentrifuge tube containing PrimeScript RT reagent mixture (TaKaRa Dalian Biotechnology, Dalian, China) according to the manufacturer's instruction. The reverse transcription was performed at 37 °C for 15 min and at 85 °C for 5 s to synthesize cDNA. Real-time PCR was then performed using iQ SYBR Green SuperMix (Bio-Rad, Hercules, CA) in a 20  $\mu$ l of reaction mixture containing 2  $\mu$ l of cDNA, 1  $\mu$ l of each primer, 6  $\mu$ l of distilled water, and 10  $\mu$ l of real time mix. The reaction was carried out in a Bio-Rad iQ5 real-time PCR system using the following parameters: 40 cycles of denaturing (94 °C, 1 min), annealing (60 °C, 30 s), and extension (72 °C, 1 min). The PCR program was completed by a melting temperature analysis. For negative controls, cDNA was replaced with water.

The primers used for *hrh2* (histamine H2 receptor gene) and  $\beta$ -*actin* were from previous reports [25, 27]. Primer sequences were as follows: *hrh2*: forward, 5'-ATG GCA TTG AAA GTC ACC-3' and reverse, 5'-GAC CAA AGA GAT GGC AAC-3';  $\beta$ -*actin*: forward, 5'-GAA ATC GTG CGT GAC ATT AAA GAG-3' and reverse, 5'-GCG GCA GTG GCC ATC TC-3'.

#### Behavioral Tests

Male rats weighing 230–250 g were used in the behavioral tests. The rats were anesthetized with sodium pentobarbital in a dose of 40 mg/kg intraperitoneally and then mounted on a stereotaxic frame (1404, David Kopf Instruments, Tujunga, CA) for brain surgery under aseptic conditions. Two stainless-steel guide tubes (length 8 mm, o.d. 0.8 mm, i.d. 0.5 mm) for the microinjection cannulae were bilaterally implanted into the cerebellum of each animal. The lower ends of guide tubes were positioned 2.0 mm above the cerebellar IN (A -11.4, L 1.8-2.2, and H 3.8), according to the rat brain atlas [24]. After the implantation, rats were caged individually and allowed to recover for at least 72 h. During the behavioral testing sessions, two stainless-steel injection cannulae (length 10 mm, o.d. 0.5 mm, i.d. 0.3 mm) were inserted to protrude

2 mm beyond the tip of the guide tube and just above the cerebellar IN (to minimize lesioning the nuclei) for microinjection of histamine (5 mM), ZD7288 (10 mM), and saline (0.9 % NaCl) using Hamilton syringes (1  $\mu$ l each side, lasting 2 min). The effective extent of the drug diffusion in the present study was restricted in the INs according to the estimate by using extracellular electrophysiological recording units 0.5–2.0 mm away from the injection site in our previous reports [2, 15].

Animals used in behavioral tests were divided into five groups: (1) sham operation, (2) microinjected with saline, (3) microinjected with histamine (dissolved in saline), (4) microinjected with ZD7288 (dissolved in saline), and (5) microinjected with histamine and ZD7288. Each animal was trained daily for at least 10 trials for three to five consecutive days in order to achieve a stable performance on the balance beam and accelerating rota-rod. All training/tests started at the same time (10:00 a.m.) each day, and each test was divided into four stages (before, 0 h, 4 h, and 24 h after microinjections).

Balance beam tests have been widely used to assess motor balance and coordination of rodents [2, 14, 15, 28]. The balance beam was a rod of 190 cm in length and a diameter of 2.5 cm. A plastic platform (7 cm  $\times$  4 cm) was placed at one end of the rod as the start, and a black plastic box (15 cm  $\times$  15 cm  $\times$  8 cm) was set at the other end of the rod as a nest for motivating the animal to cross the beam. The apparatus was suspended 90 cm above a cushion, which protected the fallen animals from injury, and 50 cm from a wall. The time taken to traverse the beam was recorded. The test consisted of five consecutive trails. To reduce stress and fatigue, the animals were allowed a 90-s rest between trials.

Accelerating rota-rod tests have also been used to assess motor balance and coordination of rodents [2, 14, 15, 28]. In this test, each rat was placed in an individual compartment of the rota-rod (Ugo Basile, Varese, Italy). Animals were first habituated to low rotation (4 rpm) for 30 s, and then the rod was evenly accelerated up to 40 rpm during 300 s. Latency for rat to fall from the rotating rod was recorded. For the test, each animal was subjected two trials, with a 3-min resting interval to reduce stress and fatigue.

### Histological Identification

On the last day of the behavioral tests, the animals were deeply anesthetized with an overdose of sodium pentobarbital, and then two insulated stainless steel wires (o.d. 0.4 mm) with 0.2 mm exposed tip were inserted (10 mm) into the cerebellar IN under guidance of guide tubes for depositing iron at the site of injection by passing DC current (10  $\mu$ A, 20 s). The brain was then removed and fixed with 4 % paraformaldehyde containing 1 % potassium ferrocyanide. A week later, frozen serial coronal sections (50  $\mu$ m thick) were prepared, performed with Nissl staining, and the dark blue dots indicating injection sites

were identified according to the rat brain atlas [24]. Data from rats in which the injection sites were deviated from the cerebellar IN were excluded from further analysis.

### Statistical Analysis

All data were analyzed with Origin 7.5 (MicroCal Software) and presented as mean  $\pm$  S.E.M. The Student's *t* test, one-way and repeated measures two-way analysis of variance (ANOVA) were employed for statistical analysis, and Newman-Keuls post hoc testing was used to further determine the differences between group means. *P* values of  $<0.05$  were considered to be significant.

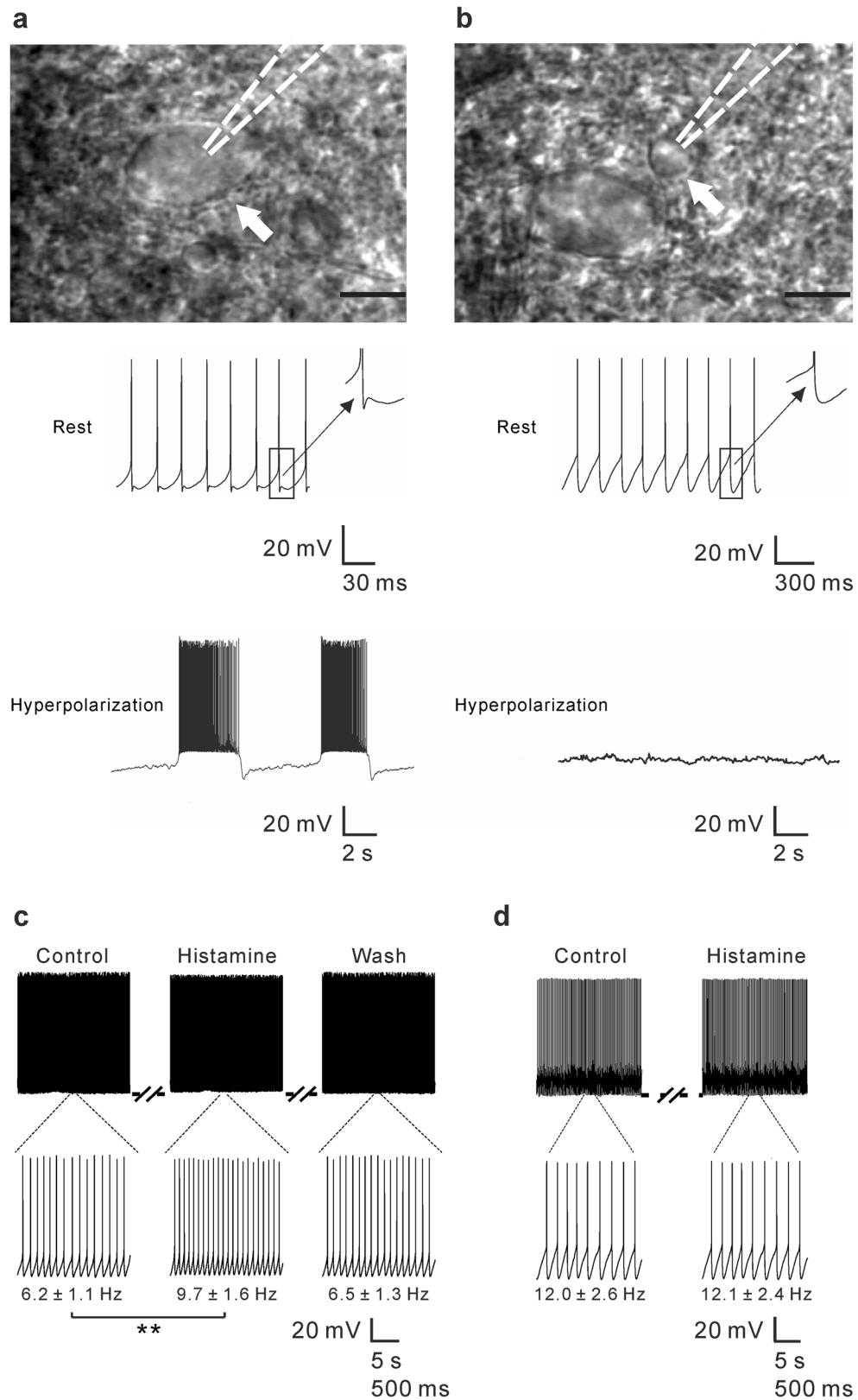
## Results

### Histamine Selectively Excites Cerebellar Nuclear Projection Neurons but Not Interneurons

We carried out whole-cell patch clamp recordings in neurons in all three cerebellar nuclei, the FN, IN, and DN, by using rat brain slices preparations. We recorded a total of 61 neurons in the cerebellar FN, IN, and DN with their membrane resistance higher than 150 M $\Omega$ . All of these recorded neurons were spontaneously active with tonic firing pattern, which is comparable with the previous reports [21, 29].

According to the different electrophysiological properties combined with morphological characteristics, we identified and categorized all recorded cerebellar nuclear neurons into two classifications, projection neurons and interneurons, similar to the previous studies [21–23]. Firstly, based on infrared differential interference contrast images obtained before whole-cell patch clamp recordings, neurons in the cerebellar nuclei with diameters  $>20$  or  $<10$   $\mu$ m were chosen and preliminarily classified as the projection neurons or interneurons, respectively (Fig. 1a, b). Subsequently, electrophysiological

**Fig. 1** Selective excitatory effect of histamine on projection neurons but not interneurons in the cerebellar nuclei. **a** Morphological and electrophysiological identifications of projection neurons in the cerebellar nuclei. Recorded neurons with the diameter larger than 20  $\mu$ m; the membrane capacitance ( $C_m$ ) higher than 150 pF; the spontaneous action potential showing a complex waveform of afterpotentials marked by a fast afterhyperpolarization (AHP), an afterdepolarization, and then a slow AHP when at rest; and the firing pattern shifted from tonic to bursting when injected continuous intracellular hyperpolarizing current were classified as projection neurons. **b** On the contrary, neurons with the diameter smaller than 10  $\mu$ m, the  $C_m$  lower than 40 pF, the afterpotential only showing a slow AHP when at rest, and the firing slowed down and finally stopped under constant hyperpolarization were categorized as interneurons. **c** Histamine (100  $\mu$ M) increased the firing rate of the projection neuron showed in **a**. **d** Histamine (100  $\mu$ M) did not influence the firing rate of the interneuron exhibited in **b**



features of the recorded neurons were carefully analyzed. A large-sized neuron (diameters  $>20 \mu\text{m}$ ) with the following

three properties was identified as a projection neuron (Fig. 1a): (i) its membrane capacitance ( $C_m$ ) was higher than

150 pF; (ii) when at rest, its spontaneous action potential showed a complex waveform of afterpotentials, marked by a fast afterhyperpolarization (AHP), an afterdepolarization, and then a slow AHP; (iii) under continuous intracellular injection of hyperpolarizing current, its spontaneous regular tonic firing pattern was shifted to bursts of high-rate firing that were separated from each other by intervals of quiescence. On the contrary, a small-sized neuron (diameters <10  $\mu\text{m}$ ) with the other three features as follows was included in the interneurons (Fig. 1b): (i) its  $C_m$  was lower than 40 pF; (ii) when at rest, its afterpotential only exhibited a slow AHP; (iii) under constant hyperpolarization, its firing slowed down and finally stopped rather than changed pattern. In fact, all large-sized neurons we recorded in this study exhibited the above-mentioned electrophysiological characteristics of the projection neurons, whereas all small ones showed electrophysiological features of interneurons.

Next, we carried out current-clamp recordings to examine the effects of histamine on projection neurons and interneurons in the cerebellar nuclei. Intriguingly, histamine exhibits a selective effect on cerebellar nuclear neurons, i.e., we found that histamine only excites projection neurons (41 of 41, 100 %) but has no effect on interneurons (0 of 12, 0 %). As shown in Fig. 1c, d, 100  $\mu\text{M}$  histamine significantly increased the firing rate of projection neurons (mean firing rate before and peak firing rate after application of histamine were  $6.2 \pm 1.1$  and  $9.7 \pm 1.6$  Hz, respectively,  $n=5$ ;  $P<0.01$ ) (Fig. 1c), but did not affect firing of those interneurons (mean firing rate before and peak firing rate after application of histamine were  $12.0 \pm 2.6$  and  $12.1 \pm 2.4$  Hz, respectively,  $n=6$ ;  $P=0.86$ ) (Fig. 1d), strongly suggesting a selective excitatory effect of histamine on cerebellar nuclear projection neurons rather than interneurons.

We further used TTX to determine whether the histamine-induced excitation on projection neurons was a direct postsynaptic effect. As shown in Fig. 2a, b, when perfusing the slices with ACSF containing 0.3  $\mu\text{M}$  TTX, although neuronal firing was impeded by TTX, 10, 30, and 100  $\mu\text{M}$  histamine still evoked a strong membrane depolarization of  $3.78 \pm 0.51$ ,  $5.32 \pm 0.40$ , and  $7.17 \pm 0.34$  mV on the cerebellar nuclear projection neurons ( $n=9$ ) in a concentration-dependent manner, indicating that histamine-induced excitation on projection neurons was evoked by directly depolarizing postsynaptic membrane, presumably through its action on the postsynaptic histamine receptors. On the other hand, 100  $\mu\text{M}$  histamine did not affect the membrane potentials of interneurons (membrane potentials before and after application of histamine were  $-49.73 \pm 1.35$  and  $-49.57 \pm 1.49$  mV, respectively;  $n=6$ ,  $P=0.38$ ) (Fig. 2c), confirming a selective excitatory effect of histamine on cerebellar nuclear neurons. Furthermore, 50  $\mu\text{M}$  gabazine (selective GABA<sub>A</sub> receptor antagonist) combined 1 mM kynurenate (ionotropic glutamate receptor antagonist) still did not influence the histamine-elicited depolarization on

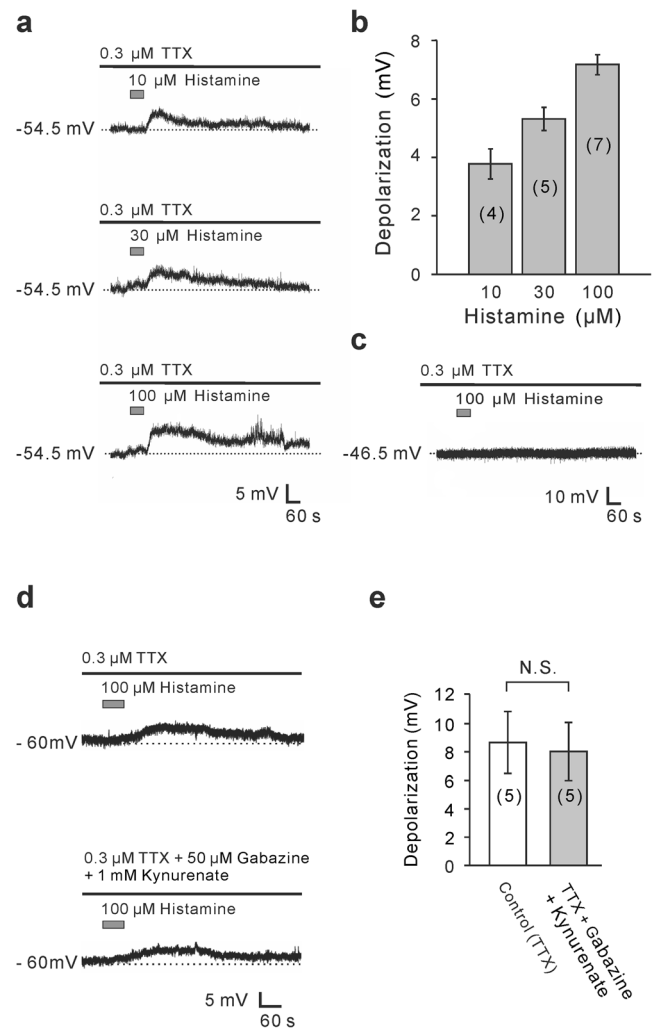


**Fig. 2** Histamine-elicited excitation on cerebellar nuclear projection neurons was due to a direct depolarization of membrane potentials. **a** Histamine dose-dependently depolarized membrane potentials on a projection neuron when application of TTX. **b** Group data of nine tested projection neurons. **c** Histamine did not influence membrane potentials of an interneuron. **d** Gabazine (GABA<sub>A</sub> receptor antagonist) and kynurenate (ionotropic glutamate receptor antagonist) did not influence the histamine-evoked depolarization on a projection neuron in TTX. **e** Group data of five tested projection neurons. Values are presented as mean  $\pm$  SEM. *n.s.* indicates non-significant

projection neurons in TTX (membrane potentials before and after application of gabazine and kynurenate were  $8.60 \pm 2.17$  and  $7.98 \pm 2.03$  mV, respectively;  $n=5$ ,  $P=0.449$ ; Fig. 2d, e). These results substantially demonstrate that the selective excitation of histamine on projection neurons in the cerebellar nuclei is a direct postsynaptic action.

#### Selective Depolarization of Histamine on Cerebellar Nuclear Neurons is Due to Exclusive Expression of H2 Receptors on Projection Neurons

To clarify why the effects of histamine on cerebellar nuclear neurons are selective, first we determined the receptor

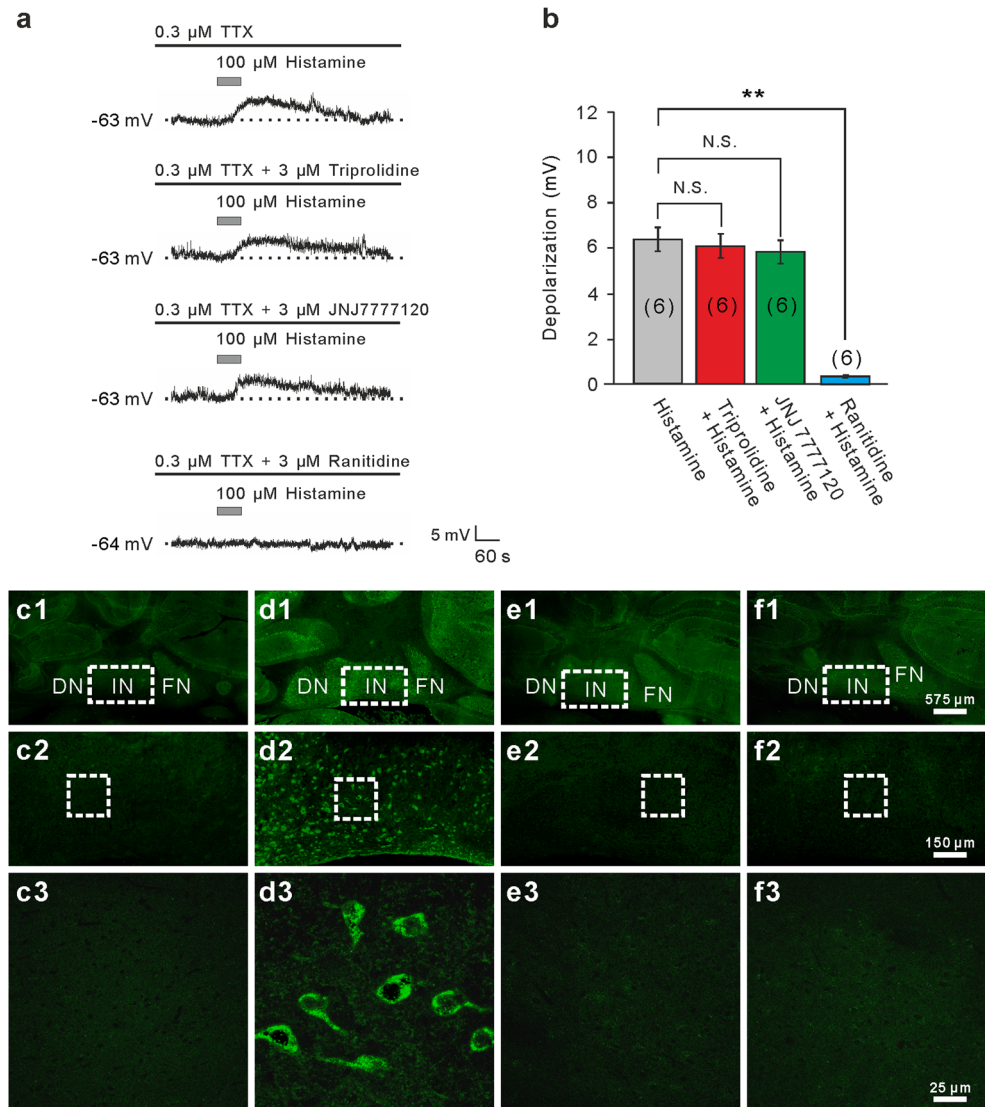
mechanism underlying the histamine-induced excitation on projection neurons. Given that depolarization induced by histamine on projection neurons is a direct postsynaptic effect, we focused on all three histamine postsynaptic receptors, H1, H2, and H4 receptors, in this study. We found that histamine-evoked depolarization on cerebellar nuclear projection neurons ( $n=6$ ) was effectively blocked by ranitidine (3  $\mu\text{M}$ ), a selective H2 receptor antagonist, but not affected by triprolidine (3  $\mu\text{M}$ ) and JNJ777120 (3  $\mu\text{M}$ ), the selective antagonists for H1 and H4 receptor, respectively. As shown in Fig. 3a, b, histamine-evoked depolarization before and after bathing triprolidine, ranitidine, and JNJ777120 were  $6.40 \pm 0.52$  mV,  $6.10 \pm 0.53$  mV ( $P=0.13$ ),  $0.35 \pm 0.05$  mV ( $P<0.01$ ), and  $5.87 \pm 0.51$  mV ( $P=0.072$ ), respectively. These results demonstrate that H2 but not H1 and H4 receptors mediate the postsynaptic excitatory effect of histamine on projection neurons, which are consistent with our previous extracellular

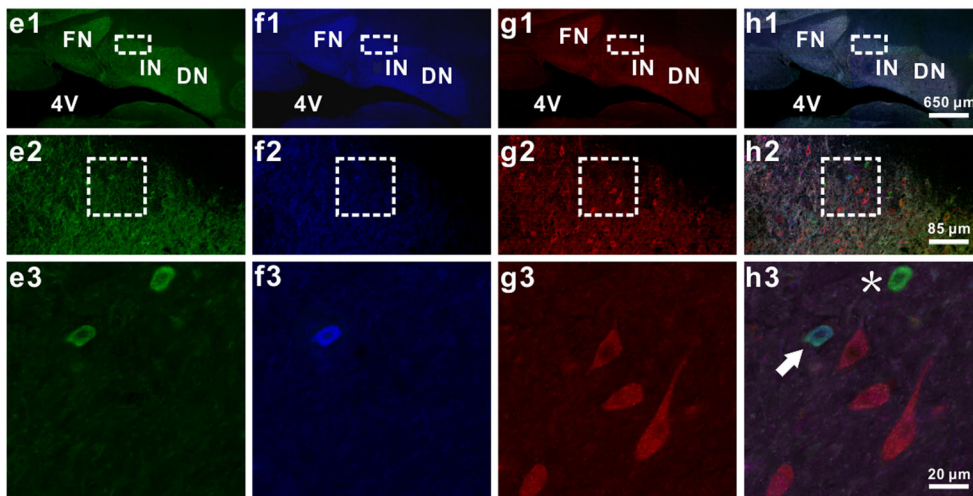
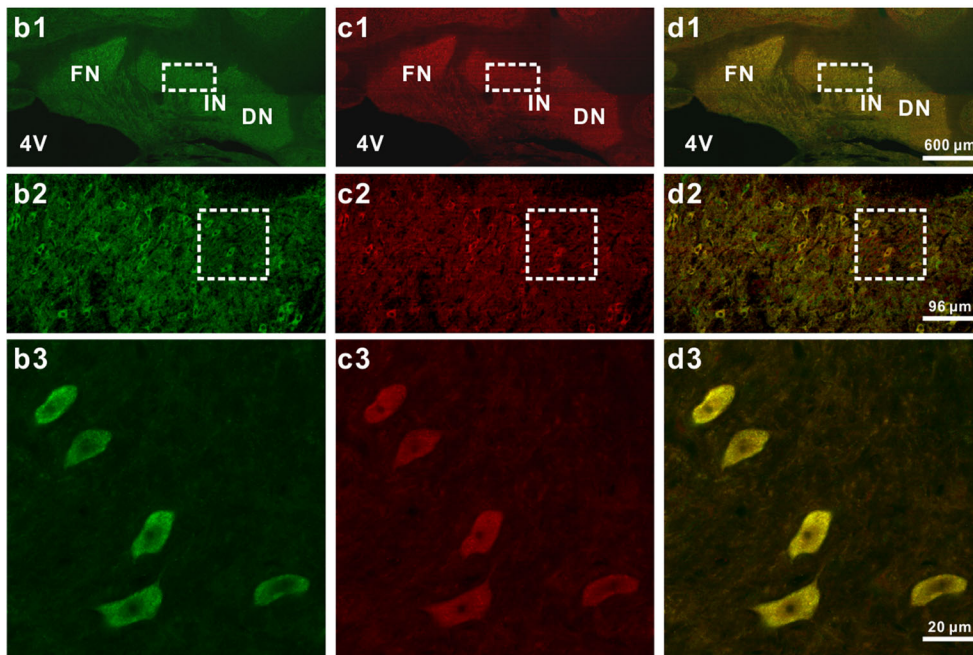
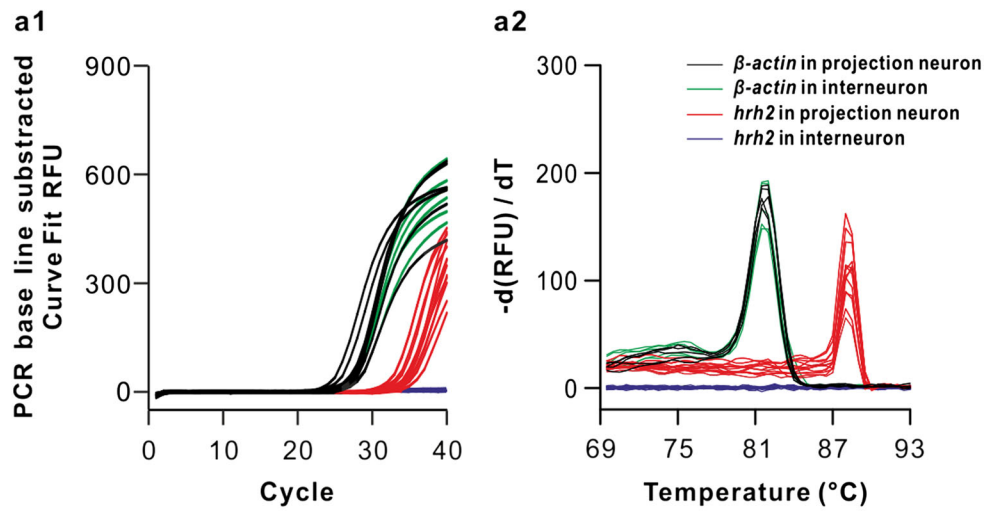
recordings [1, 14]. Furthermore, immunostaining results showed that H2 rather than H1 and H4 receptors were present in the rat cerebellar nuclei (Fig. 3(c1–f3)), confirming that only H2 receptors were involved in histamine-induced excitation.

Next, we employed single-cell RT-PCR to assess whether H2 receptor mRNAs are selectively expressed in the recorded projection neurons but not interneurons in the cerebellar nuclei. Interestingly, amplification and melting temperature curves of *hrh2* and  $\beta$ -actin (the control housekeeping gene) in projection neurons ( $n=6$ ) and interneurons ( $n=7$ ) show that H2 receptor mRNAs are only expressed in projection neurons rather than interneurons (Fig. 4(a1, a2)), which is consistent with the above electrophysiological data.

Although there is still no precise markers for identifying projection and interneurons in the cerebellar nuclei, it has been well known that cerebellar nuclear projection neurons are

**Fig. 3** Histamine H2 receptors mediate the histamine-induced depolarization on cerebellar nuclear projection neurons and the expression of postsynaptic histamine receptors in the cerebellar nuclei. **a** Ranitidine, a selective H2 receptor antagonist, instead of triprolidine and JNJ777120, selective antagonists for H1 and H4 receptor, blocked the histamine-induced depolarization on a projection neuron. **b** Group data of six tested projection neurons. Values are presented as mean  $\pm$  SEM. *n.s.* indicates non-significant and  $** P<0.01$ . *c1–e3* Immunostainings for H1 (*c1–c3*), H2 (*d1–d3*), and H4 (*e1–e3*) receptors in the rat cerebellar nuclei. *f1–f3* Negative staining control by omitting the primary antiserum. Note that only H2 receptor immunostainings were present in all three cerebellar nuclei. *DN*, dentate nucleus; *FN*, fastigial nucleus; *IN*, interpositus nucleus







◀ **Fig. 4** Histamine H2 receptors selectively expressed and localized in the glutamatergic projection neurons in the cerebellar interpositus nucleus (IN). *a1* Amplification curves for *hrh2* and  $\beta$ -actin were obtained to identify the cycle thresholds ( $C_t$ ) at which receptor fluorescence intensity significantly exceeded background fluorescence signals. Note that each curve corresponds to the template mRNAs from a single projection neuron or interneuron. *a2* A melting temperature curve analysis was performed to determine that the reactions yielded only one product per gene. Each peak corresponds to the melting temperature of *hrh2* and  $\beta$ -actin. Note that histamine H2 receptor mRNAs are only expressed in projection neurons rather than interneurons. *b1–d3* Double immunostainings showed that VGLUT2 (*b1–b3*) and histamine H2 receptors (*c1–c3*) were not only present in the rat IN but also colocalized in the same neurons (*d1–d3*), indicating an expression of H2 receptors on IN glutamatergic projection neurons. *e1–h3* Triple immunostainings showed that H2 receptors (*g1–g3*) did not localize in neurons expressing GAD67 (*e1–e3*) and GLYT2 (*f1–f3*), indicating H2 receptors were not expressed on GABAergic neurons (projection or interneurons, indicated by *asterisk*) and GABA/glycinergic interneurons (indicated by *arrow*) in the IN (*h1–h3*). *4 V*, 4th ventricle; *DN*, dentate nucleus; *FN*, fastigial nucleus; *IN*, interpositus nucleus

glutamatergic, GABAergic, or glycinergic (glycinergic ones are only reported in the FN and DN in mice) [16, 30–32], whereas interneurons are GABAergic and/or glycinergic [16, 33]. Therefore, in the present study, we used anti-H2 receptor antibody, together with anti-vesicular glutamate transporter VGLUT2, or anti-GAD67 (a key enzyme in GABA biosynthesis) and anti-glycine transporter GLYT2 antibodies to colabel the cerebellar nuclear neurons, and observed the expression and distribution of H2 receptors in glutamatergic, GABAergic, and glycinergic neurons in all three cerebellar nuclei. In the cerebellar IN, as shown in Fig. 4(b1–d3, e1–h3), H2 receptors were only localized and present in glutamatergic neurons rather than GABAergic and GABA/glycinergic ones. Since cerebellar IN projection neurons contain large-sized glutamatergic neurons and medium-sized GABAergic ones, whereas interneurons consist of small- and medium-sized GABAergic and GABA/glycinergic neurons, the results suggest that H2 receptors are restrictedly expressed on glutamatergic projection neurons but not GABAergic projection neurons, GABAergic interneurons, or GABA/glycinergic interneurons in the IN. We also observed a similar expression and localization of H2 receptors in the cerebellar DN (Fig. S1).

In the rat cerebellar FN, we found that large projection neurons include both glutamatergic and glycinergic ones, in which the formers are mostly located in the dorsal part, whereas the latters are predominately located in the ventral and intermediate part. As shown in Fig. 5, H2 receptors were expressed in both of them (Fig. 5(a1–c3, d1–g3)), however, did not localize in the GABAergic and GABA/glycinergic neurons (Fig. 5(h1–k3)). All these results indicate that H2 receptors are exclusively expressed and distributed in projection neurons, primarily glutamatergic and glycinergic (only in the ventral and intermediate part of FN), but not interneurons,

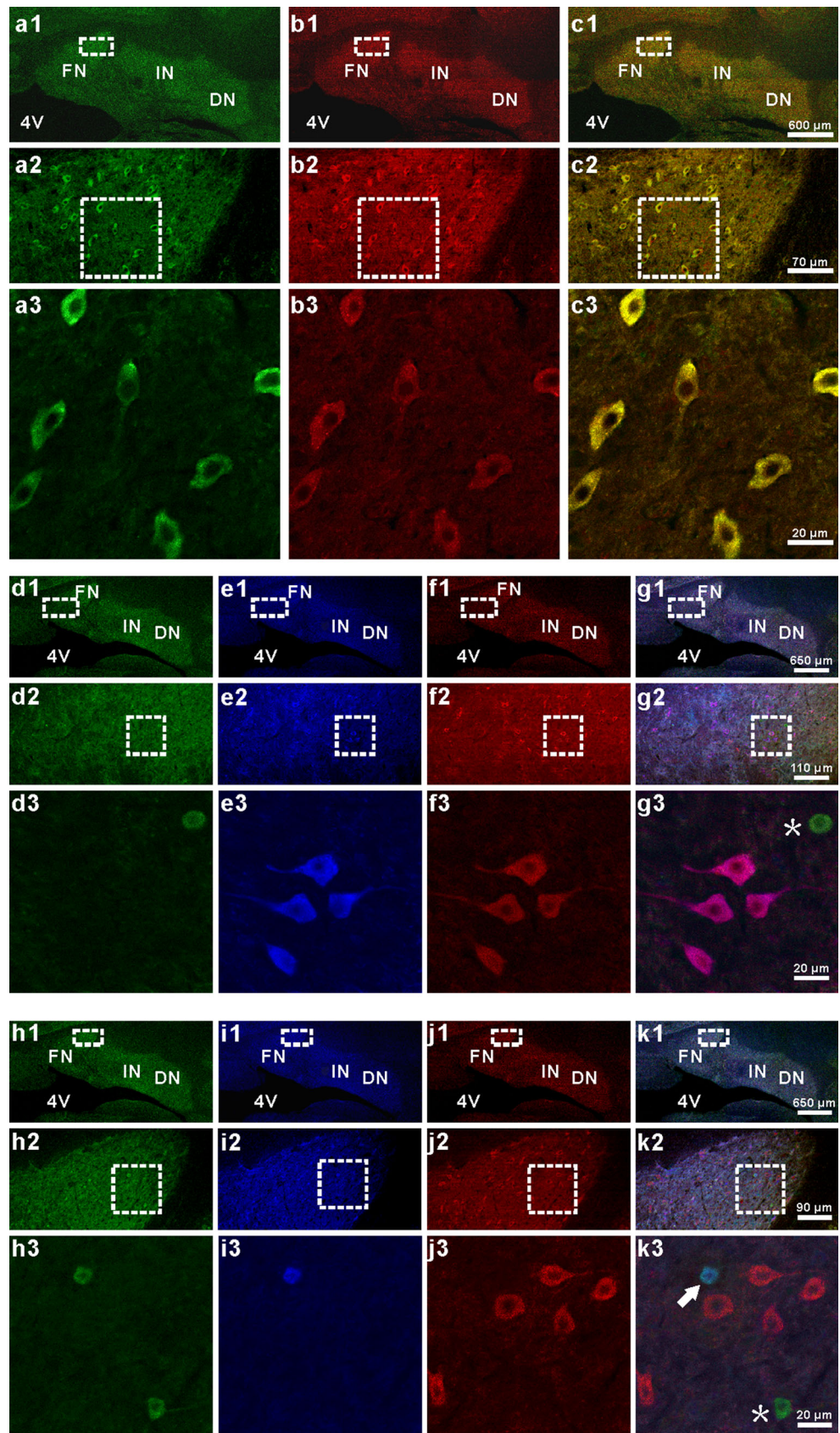
accounting for a selective role of histamine in cerebellar nuclei.

#### HCN Channels Underlies the Histamine-Evoked Depolarization on Cerebellar Nuclear Projection Neurons

It has been reported that two downstream ionic mechanisms, HCN channel and  $\text{Ca}^{2+}$ -activated  $\text{K}^+$  conductance [3, 4], are involved in neuronal excitation following histamine H2 receptor activation. To evaluate the ionic basis underlying histamine-induced excitation on cerebellar nuclear projection neurons, we first examined the change of input resistance when histamine induced neuronal depolarization. As shown in Fig. 6(a1, a2), a step current (ranging from  $-90$  to  $-200$  pA in 10 pA steps) was run to acquire a series of corresponding membrane voltage changes, and then an  $I$ - $V$  curve was fitted by linear regression. At rest, the mean membrane resistance of eight recorded projection neurons was  $280.8 \pm 44.3$  M $\Omega$ . Comparing the  $I$ - $V$  curves before and after application of 30 and 100  $\mu\text{M}$  histamine, we found a slight decrease of the membrane resistance accompanying the histamine-evoked depolarization ( $22.25 \pm 3.74$  and  $29.74 \pm 2.60$  % of the control,  $n=5$ ; Fig. 6(a3)), indicating that histamine caused an opening of ion channels in the membrane of cerebellar nuclear projection neurons.

Notably, during the course of negative voltage deviations induced by hyperpolarizing current stimulation, the depolarizing voltage sag, one of the hallmarks of HCN channels, is generated (Fig. 6(a1)), indicating that HCN channels may be involved in the depolarization of histamine on projection neurons in the cerebellar nuclei. To address this issue, we carried out a protocol of a series of 1 s hyperpolarizing voltage steps (ranging from  $-50$  to  $-120$  mV in 10 mV steps) [26, 34, 35] to determine the effect of histamine on HCN channel current. As shown in Fig. 6(b1–b4), in the presence of TTX (0.5  $\mu\text{M}$ ) and  $\text{BaCl}_2$  (100  $\mu\text{M}$ ), histamine (100  $\mu\text{M}$ ) induced a significant increment in instantaneous current ( $I_{\text{Ins}}$ ) at step potentials less than  $-80$  mV ( $P < 0.05$ ,  $n=6$ ; Fig. 6(b2)) and in maximum current at 1 s ( $I_{\text{Max-1s}}$ ) at step potentials less than  $-70$  mV ( $P < 0.05$  and 0.01,  $n=6$ ; Fig. 6(b3)); ZD7288 (50  $\mu\text{M}$ ), a selective blocker for HCN channels, totally blocked histamine-induced increment in  $I_{\text{Ins}}$  at step potentials less than  $-70$  mV ( $P < 0.05$  and 0.01,  $n=6$ ; Fig. 6(b2)) and a  $I_{\text{Max-1s}}$  at step potentials less than  $-60$  mV ( $P < 0.05$  and 0.01,  $n=6$ ; Fig. 6(b3)). In fact, the HCN channel current ( $I_{\text{Max-1s}} - I_{\text{Ins}}$ ) that was activated at step potentials less than  $-60$  mV in cerebellar nuclear projection neurons (Fig. 6(b4)) was significantly increased by histamine and blocked by ZD7288 (Fig. 6(b4)). Furthermore, we applied ZD7288 (50  $\mu\text{M}$ ) to block the HCN channel in current-clamp recordings and found that the histamine-evoked depolarization was nearly totally blocked ( $0.83 \pm 0.18$  vs  $5.63 \pm 0.34$  mV of the control,  $P < 0.01$ ; Fig. 6(c1, c2)). All these results strongly suggest that

**Fig. 5** Histamine H2 receptors selectively expressed and localized in the glutamatergic projection neurons in dorsal part of the cerebellar fastigial nuclei (FN) and glycinergic projection neurons in the ventral and intermediate part of FN. *a1–c3* Double immunostainings showed that VGLUT2 (*a1–a3*) and histamine H2 receptors (*b1–b3*) were not only present in the dorsal part of rat FN but also co-localized in the same neurons (*c1–c3*), indicating an expression of H2 receptors on dorsal FN glutamatergic projection neurons. *d1–g3* Triple immunostainings showed that H2 receptors (*f1–f3*) localize in neurons expressing GLYT2 (*e1–e3*) but not GAD67 (*d1–d3*) in the ventral and intermediate part of FN, indicating H2 receptors were also expressed on glycinergic projection neurons rather than GABAergic neurons (projection or interneurons, indicated by *asterisk*) in the ventral and intermediate FN (*g1–g3*). *h1–k3* Triple immunostainings showed that H2 receptors (*j1–j3*) did not localize in dorsal FN neurons expressing GAD67 (*h1–h3*) and GLYT2 (*i1–i3*), suggesting GABAergic neurons (indicated by *asterisk*) and GABA/glycinergic interneurons (indicated by *arrow*) in the dorsal FN did not express H2 receptors (*k1–k3*). *4V*, 4th ventricle; *DN*, dentate nucleus; *FN*, fastigial nucleus; *IN*, interpositus nucleus



HCN channels underlie the histamine-induced depolarization on cerebellar nuclear projection neurons.

Given that small conductance  $\text{Ca}^{2+}$ -activated  $\text{K}^+$  (SK) channels are also coupled to histamine H2 receptor activation in other brain regions [36], we further investigated whether closure of SK channels is involved in the histamine-induced excitation on cerebellar nuclear projection neurons ( $n=6$ ). Since SK channels are active at the resting potential of cerebellar nuclear projection neurons [37] and responsible for neuronal intrinsic firing [38], the effect of histamine on firing rates after blocking HCN channels was observed. As shown in Fig. 6(d1, d2), 50  $\mu\text{M}$  ZD7288, blocking HCN channels, slightly decreased the firing rate of the cerebellar nuclear projection neurons (mean firing rates before and after perfusing ZD7288 are  $8.45 \pm 1.10$  and  $7.27 \pm 1.08$  Hz, respectively;  $P < 0.01$ ); however, 100  $\mu\text{M}$  histamine did not influence the firing rate after HCN channels were blocked (mean firing rate before and after application of histamine were  $7.27 \pm 1.08$  and  $7.28 \pm 1.08$  Hz, respectively;  $P = 0.79$ ). These results suggest that HCN channels rather than SK channels contribute to histamine-induced excitation on cerebellar nuclear projection neurons.

#### Blockage of HCN Channels in the Cerebellar IN Attenuates Histamine-Induced Promotion on Motor Balance and Coordination

Since IN in the cerebellar nuclei is the primary final output node of spinocerebellum and develops later in vertebrate phylogeny for precise control of distal muscles of the limbs and digits [17, 18], we microinjected saline, histamine (5 mM), ZD7288 (10 mM), or histamine together with ZD7288 into bilateral INs to determine the effect of blockage of HCN channels on histamine-promoted motor behaviors on balance beam and accelerating rota-rod. Before microinjections, the mean score of 50 rats of all groups for the balance beam tests was  $4.42 \pm 0.04$  s, and there was no significant difference among the groups before injections ( $F_{(4, 45)} = 0.375$ ,  $P = 0.825$ ; Fig. 7a). A two-way ANOVA with repeated measures revealed a significant effect of time ( $F_{(3, 135)} = 19.127$ ,  $P < 0.01$ ), treatment ( $F_{(4, 45)} = 12.15$ ,  $P < 0.01$ ), and time  $\times$  treatment interaction ( $F_{(12, 135)} = 27.461$ ,  $P < 0.01$ ) among these groups. Furthermore, Newman-Keuls post hoc test indicated that microinjection of histamine ( $n=10$ ) into the cerebellar INs significantly shortened the time that rats spent traversing the beam at 0 h after injection compared with the saline group ( $n=10$ ) ( $P < 0.01$ , Fig. 7a), and such effect recovered hours later (Fig. 7a). Notably, the spending time after injection of group injected with histamine together with ZD7288 (blocker for HCN channels,  $n=10$ ) was remarkably longer than that of the histamine group at 0 and 4 h ( $P < 0.01$ , Fig. 7a), and shorter than that of the ZD7288 group ( $n=10$ ) at 0 h ( $P < 0.05$ , Fig. 7a). These results suggest that HCN channels in the

cerebellar IN mediate the promotive effect of histamine on motor performance on balance beam. Also, the time for rats taken to walk across the beam of the ZD7288 group was significantly more prolonged than that of the saline group at 0 and 4 h ( $P < 0.01$ , Fig. 7a), indicating blockage of endogenous histaminergic inputs in the cerebellar IN by antagonizing HCN channels attenuates motor balance and coordination on the balance beam.

In the accelerating rota-rod test, the mean score of 50 rats of all groups on the rod was  $125.64 \pm 1.53$  s, and there was no significant difference among the groups before injection ( $F_{(4, 45)} = 0.497$ ,  $P = 0.738$ ; Fig. 7b). A two-way ANOVA with repeated measures revealed a significant effect of time ( $F_{(3, 135)} = 20.330$ ,  $P < 0.01$ ), treatment ( $F_{(4, 45)} = 6.668$ ,  $P < 0.01$ ), and time  $\times$  treatment interaction ( $F_{(12, 135)} = 50.949$ ,  $P < 0.01$ ). Newman-Keuls post hoc test indicated that microinjection of histamine ( $n=10$ ) into the cerebellar IN significantly lengthened the endurance time of rats on the rotating rod 0 h ( $P < 0.01$ , Fig. 7b) and 4 h ( $P < 0.01$ , Fig. 7b) after injection compared with the saline group ( $n=10$ ). This effect was recovered hours later. It is noteworthy that the endurance time after injection of the group injected with histamine together with ZD7288 ( $n=10$ ) was remarkably shorter than that of the histamine group at 0 and 4 h ( $P < 0.01$ , Fig. 7b), and longer than that of the ZD7288 group ( $n=10$ ) at 0 h ( $P < 0.05$ , Fig. 7b), indicating that the histamine-induced improvement of motor performance is mediated by HCN channels. Moreover, in comparison with the saline ones, the endurance time for rats microinjected with ZD7288 was remarkably shortened at 0 and 4 h ( $P < 0.01$ , Fig. 7b). All these results strongly suggest that endogenous histaminergic afferent inputs promote cerebellum-mediated motor balance and coordination via activation of HCN channels.

Figure 7c, d presents the coronal Nissl-stained histological sections from the rat brain showing two injection sites in the superficial cerebellar IN: the tracts of the guide tubes above the bilateral nuclei, and the reconstructed microinjection sites within the IN ( $n=50$  in each side), respectively.

## Discussion

Movement is the basis for execution of behavior. Depletion of brain histamine or knockout of histamine receptors altered ambulatory activity and reduced locomotor activity and exploratory behavior [39–41], indicating the central histaminergic system, a general modulator for whole brain activity, may also hold a key position in somatic motor control [1]. However, its precise function and the underlying mechanism remain enigmatic. Here, we demonstrate a selective excitatory effect of histamine on projection neurons rather than interneurons in the cerebellar nuclei, the final integrative center and output of

the cerebellum, the largest subcortical motor center. This selective action is mediated by postsynaptic histamine H2 receptors, which are exclusively expressed in the cerebellar nuclear glutamatergic projection neurons and glycinergic projection neurons in the ventral and intermediate part of the FN. The downstream HCN channels coupled to H2 receptors contribute to the histamine-induced depolarization on these projection neurons and enable histamine/histaminergic inputs to exert their functional role on cerebellum-mediated motor balance and motor coordination.

#### Mechanism Underlying the Selective Effect of Histamine in Cerebellar Nuclei

Two types of neurons, the projection neurons and interneurons, orchestrate local circuitry in the cerebellar nuclei [16]. According to the morphological features and particularly the electrophysiological properties [21–23], including membrane capacitance, waveform of afterpotentials, and response to a constant hyperpolarization, we classified all the recorded neurons and found that histamine only depolarizes and excites cerebellar nuclear projection neurons rather than interneurons, suggesting a selective role of histamine in local circuit in the cerebellar nuclei. Interestingly, histamine H2 receptors, mediating the histamine-induced excitation on projection neurons, are only expressed in glutamatergic and glycinergic neurons (only in the ventral and intermediate part of FN) rather than GABAergic and GABA/glycinergic ones. Since glutamatergic and glycinergic neurons are principle projection neurons in the cerebellar nuclei, whereas GABAergic and GABA/glycinergic ones are nucleo-olivary neurons and interneurons [16, 42], the differential expression of the H2 receptors accounts for why histamine exerts a selective action on projection neurons, but not interneurons in the cerebellar nuclei.

HCN channel and SK channel are two known downstream ionic mechanisms coupled to H2 receptors in the brain [3, 4]. In this study, we find that HCN channel but not SK channel contributes to the depolarizing action of histamine on cerebellar nuclear projection neurons. The expression of four subtypes of HCN channels (HCN1, HCN2, HCN3, HCN4) in the cerebellar nuclei and the involvement of four HCN channel subtypes in excitation of histamine on cerebellar projection neurons still need further investigated. Generally, HCN channels are considered as “pacemaker channels” of neurons in the brain [43]. They are activated during hyperpolarization, and thus to help to accelerate neuronal depolarization to trigger spikes and generate rhythmic firings. Therefore, via opening of HCN channels coupled to H2 receptors, histamine can quickly increase the excitability of cerebellar nuclear projection neurons and modulate their firing. By this way, histamine/histaminergic inputs may directly regulate projection neurons rather than interneurons in the cerebellar nuclei, with the

**Fig. 6** Histamine-evoked depolarization on cerebellar nuclear projection neurons was mediated by the activation of hyperpolarization-activated cyclic nucleotide-gated (HCN) channels. *a1* A step current (ranging from  $-90$  to  $-200$  pA in 10 pA steps) was run to acquire a series of corresponding membrane voltage changes. Note that the depolarizing voltage sag, one of the hallmarks of HCN channel, was generated during the hyperpolarizing stimulation. *a2* Successful linear regression was used to generate the  $I$ - $V$  curves before and after application of histamine. The slope of the curve was calculated as the membrane resistance. *a3* Group data revealed that histamine dose-dependently reduced the membrane resistance of five tested projection neurons, indicating that histamine caused an opening of ion channels. *b1* A series of 1 s hyperpolarizing voltage steps (ranging from  $-50$  to  $-120$  mV in 10 mV steps) were employed to observe the effect of histamine (100  $\mu$ M), ZD7288 (50  $\mu$ M), and histamine (100  $\mu$ M) together with ZD7288 (50  $\mu$ M) on the current of HCN channel. *b2–b4* Plots of instantaneous current ( $I_{\text{Ins}}$ , *b2*), maximum current at 1 s ( $I_{\text{Max-1s}}$ , *b3*), and HCN channel current ( $I_{\text{Max-1s}}-I_{\text{Ins}}$ , *b4*) in the control and during the application of histamine, ZD7288, and histamine together with ZD7288 against the membrane potential. The *black asterisks* indicate significances between histamine group and the control, whereas *green asterisks* indicate significances between histamine group and histamine together with ZD7288 group. *c1* ZD7288, a selective blocker for HCN channels, nearly totally blocked the histamine-evoked depolarization on a projection neuron. *c2* Group data of five tested projection neurons. *d1* Histamine did not influence the firing rate after HCN channels were blocked, although ZD7288 slightly decreased the firing rate. *d2* Group data of six tested projection neurons. Values are presented as mean  $\pm$  SEM. *n.s.* indicates non-significant, \* $P < 0.05$  and \*\* $P < 0.01$

avoidance of redundant processing in the local circuit, to realize a prompt modulation on the ultimate outputs of the cerebellum.

#### Physiological Significance of Selective Modulation of Histamine on Projection Neurons in Cerebellar Nuclei

In the cerebellar circuitry, the glutamatergic projection neurons of the cerebellar nuclei produce the principle output of the cerebellum [16]. Thus, the excitatory modulation of histamine on cerebellar nuclear glutamate projection neurons will enhance the final cerebellar output and excite their targets. On the other hand, two types of glycinergic projection neurons exist in the cerebellar nuclei: one consists of spontaneously active neurons in the FN projecting to the vestibular nuclei [32], and another is formed by silent ones which target the cerebellar cortical granule cells [44]. Since granule cells receive inputs from mossy fibers and their axons form parallel fibers to excite Purkinje cells, histamine-induced excitation on these silent cerebellar nuclear glycinergic projection neurons will inhibit glutamatergic granule cells and GABAergic Purkinje cells, and eventually result in excitation of cerebellar nuclear neurons.

In fact, the effect of histamine on motor behaviors mediated through cerebellar nuclear circuitry is highly in agreement with the above theoretical expectation of the selective activation of these cerebellar nuclear projection neurons by histamine, although the behavioral effect of excitation of FN

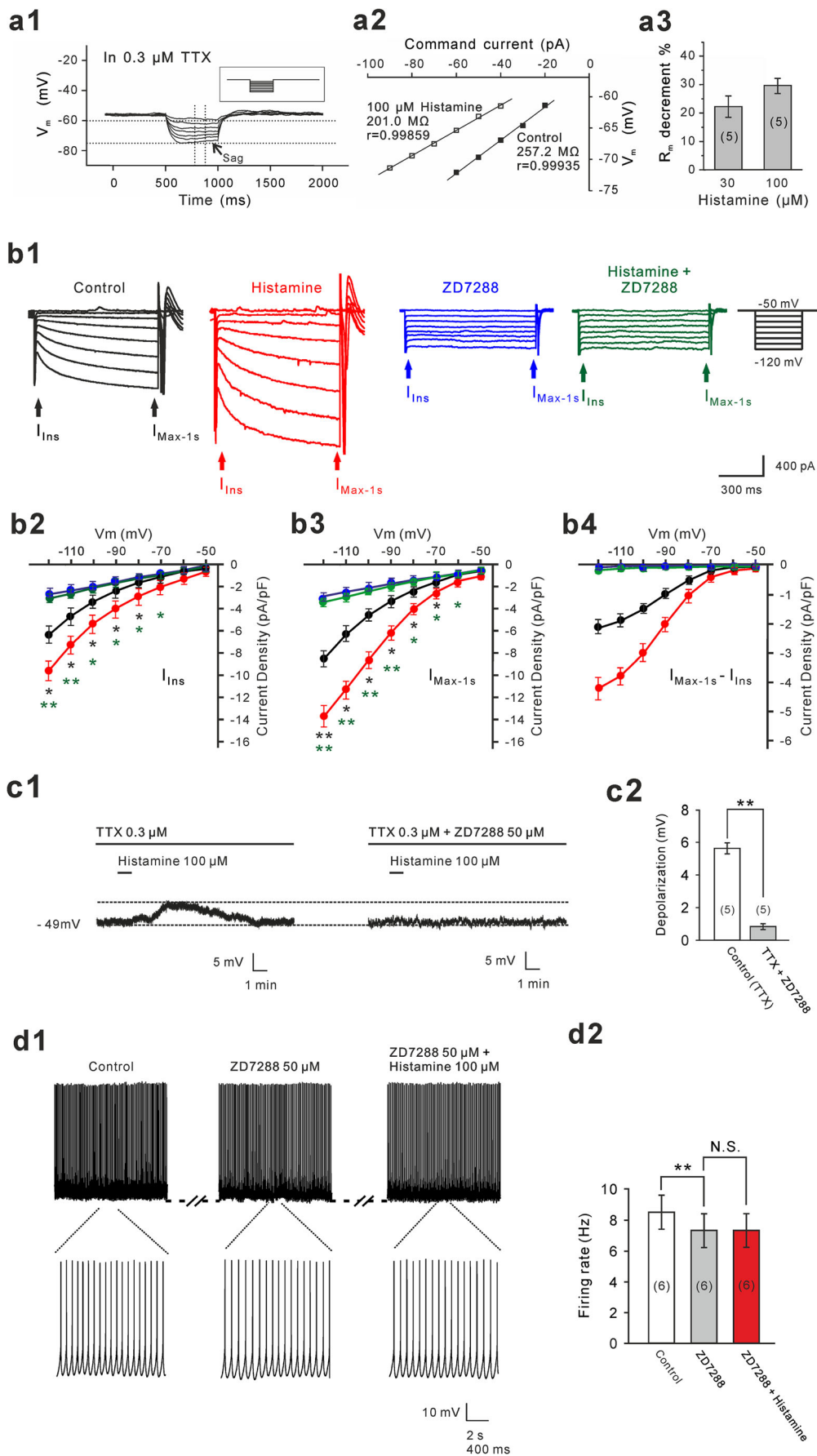
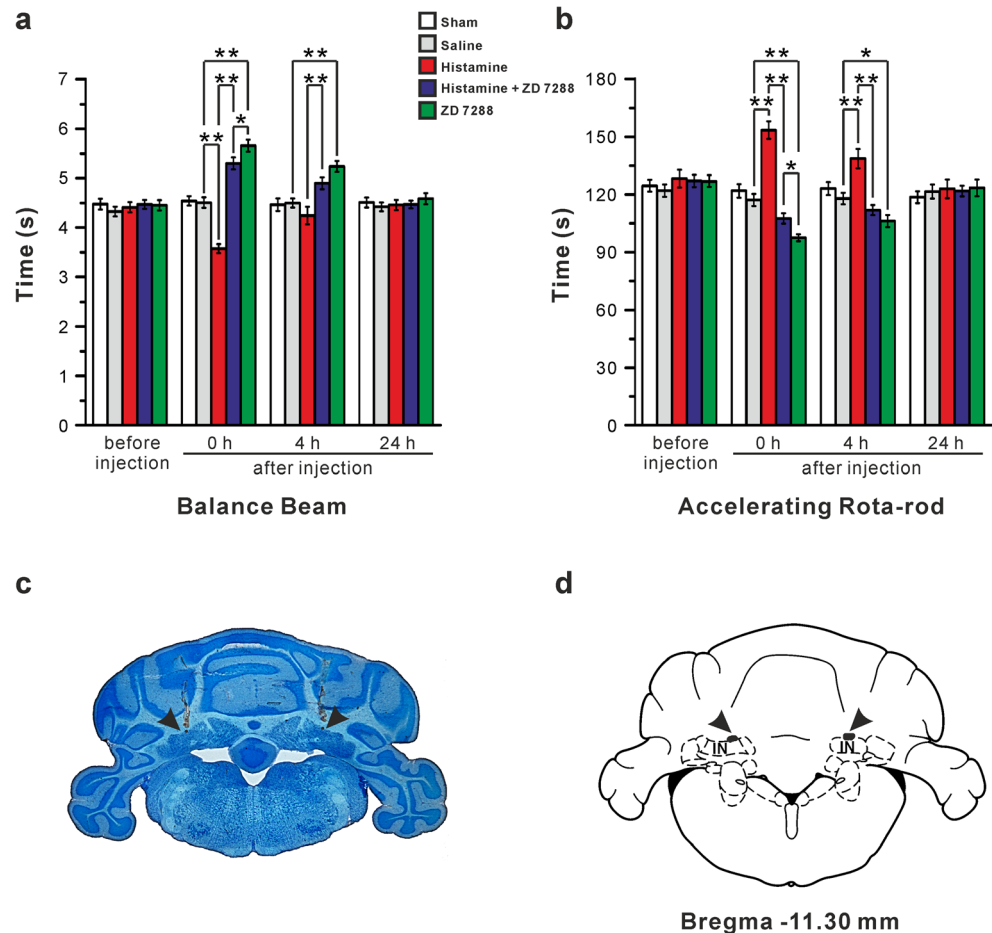


**Fig. 7** Blockage of HCN channels in the cerebellar interpositus nuclei (IN) attenuates histamine-induced promotion on motor balance and coordination. **a, b** The duration of passage through the balance beam and the endurance time on an accelerating rota-rod of sham operated rats and rats treated by bilateral microinjection of saline, histamine, ZD7288, or histamine together with ZD7288. **c** A coronal section (50  $\mu\text{m}$  in thickness) of rat cerebellum showing the sites of microinjection within the superficial IN (indicated by the *arrowhead*). The bloodstain presented the traces of guide tubes that were positioned 2 mm above the IN. **d** Histological reconstruction showing the microinjections sites (indicated by the *arrowhead*) across 50 animals



glycinergic neurons targeting the vestibular nuclei is still unclear. In our previous [14, 15, 45] and the present studies, we found that microinjection of histamine into the superficial part of the cerebellar nuclei (both the FN and IN) remarkably promotes motor balance and coordination on accelerating rota-rod and balance beam. Importantly, blockage of HCN channels, the final site of histamine-evoked intracellular signal transduction, to block the action of histaminergic inputs on the cerebellar IN significantly attenuates motor performances, suggesting endogenous histamine is critical for cerebellar motor control. Considering the hypothalamocerebellar histaminergic inputs are direct, monosynaptic projection [6] and HCN channel is responsible for neuronal excitability, we suggest that endogenous histamine and histaminergic inputs may act as a rapid biasing force to influence electrophysiological properties of cerebellar nuclear projection neurons and hold their excitability at an appropriate level for responding to concrete inputs coding changes in internal and external environments.

More importantly, distinguished from selective action of histamine on interneurons in substantia nigra [46], neostriatum [47], and ventral tegmental areas [46], the biasing effect of histamine on final outputs of the cerebellar circuitry is orchestrated through direct and quick modulation on projection neurons in the cerebellar nuclei. The direct innervation

and modulation of histaminergic inputs on cerebellar nuclear projection neurons rather than interneurons may help the cerebellum to make a rapid reaction to both of the central motor command and peripheral feedback signals, so that a quick cerebellar regulation on ongoing movements can be achieved.

Despite being a third type of cerebellar afferents, histaminergic afferents in the cerebellum may differ from the serotonergic and noradrenergic fibers arising from the brainstem. Since originating from the hypothalamus, a higher center for visceral and autonomic regulation, the hypothalamocerebellar histaminergic projections bridge nonsomatic center to somatic structure. These histaminergic modulations may not only endow the cerebellar circuitry with an appropriate functional state but also form a vital part of the somatic-nonsomatic integration, which is critical for generating an integrated and coordinated behavioral response to changes in internal and external environment. Through the direct modulation on projection neurons, primarily glutamatergic ones, in the cerebellar nuclei, hypothalamocerebellar histaminergic inputs may not only quickly regulate ongoing movement but also realize a rapid integration of somatic and nonsomatic responses, which is substantially needed for an integrated and coordinated behavior.

**Acknowledgments** We thank Dr Rob Leurs (VU University Amsterdam, Amsterdam, the Netherlands) for his generous gifts of histamine H4 receptor agonist and antagonist. The work was supported by grants 31070959, 31071021, 31171050, 31330033, 91332124, 31471112 and NSFC/RGC Joint Research Scheme 31461163001 from the National Natural Science Foundation of China; SRFDP/RGC ERG grant 20130091140003 and NCET Program from the State Educational Ministry of China; grants BK2011014 and BK20140599 from the Natural Science Foundation of Jiangsu Province, China; and grant 2013T60520 from the China Postdoctoral Science Foundation.

**Conflict of Interest** None.

## References

- Zhu JN, Yung WH, Kwok-Chong Chow B, Chan YS, Wang JJ (2006) The cerebellar-hypothalamic circuits: potential pathways underlying cerebellar involvement in somatic-visceral integration. *Brain Res Rev* 52(1):93–106
- Zhang J, Li B, Yu L, He YC, Li HZ, Zhu JN, Wang JJ (2011) A role for orexin in central vestibular motor control. *Neuron* 69(4):793–804
- Haas H, Panula P (2003) The role of histamine and the tuberomammillary nucleus in the nervous system. *Nat Rev Neurosci* 4(2):121–130
- Haas HL, Sergeeva OA, Selbach O (2008) Histamine in the nervous system. *Physiol Rev* 88(3):1183–1241
- Dietrichs E (1984) Cerebellar autonomic function: direct hypothalamocerebellar pathway. *Science* 223(4636):591–593
- Haines DE, Dietrichs E, Mihailoff GA, McDonald EF (1997) The cerebellar-hypothalamic axis: basic circuits and clinical observations. *Int Rev Neurobiol* 41:83–107
- Panula P, Pirvola U, Auvinen S, Airaksinen MS (1989) Histamine-immunoreactive nerve fibers in the rat brain. *Neuroscience* 28(3):585–610
- Panula P, Takagi H, Inagaki N, Yamatodani A, Tohyama M, Wada H, Kotilainen E (1993) Histamine-containing nerve fibers innervate human cerebellum. *Neurosci Lett* 160(1):53–56
- Airaksinen MS, Panula P (1988) The histaminergic system in the guinea pig central nervous system: an immunocytochemical mapping study using an antiserum against histamine. *J Comp Neurol* 273(2):163–186
- Arrang JM, Drutel G, Garbarg M, Ruat M, Traiffort E, Schwartz JC (1995) Molecular and functional diversity of histamine receptor subtypes. *Ann N Y Acad Sci* 757:314–323
- Vizuete ML, Traiffort E, Bouthenet ML, Ruat M, Souil E, Tardivel-Lacombe J, Schwartz JC (1997) Detailed mapping of the histamine H2 receptor and its gene transcripts in guinea-pig brain. *Neuroscience* 80(2):321–343
- Honrubia MA, Vilaro MT, Palacios JM, Mengod G (2000) Distribution of the histamine H(2) receptor in monkey brain and its mRNA localization in monkey and human brain. *Synapse* 38(3):343–354
- Karlstedt K, Senkas A, Ahman M, Panula P (2001) Regional expression of the histamine H(2) receptor in adult and developing rat brain. *Neuroscience* 102(1):201–208
- He YC, Wu GY, Li D, Tang B, Li B, Ding Y, Zhu JN, Wang JJ (2012) Histamine promotes rat motor performances by activation of H(2) receptors in the cerebellar fastigial nucleus. *Behav Brain Res* 228(1):44–52
- Song YN, Li HZ, Zhu JN, Guo CL, Wang JJ (2006) Histamine improves rat rota-rod and balance beam performances through H(2) receptors in the cerebellar interpositus nucleus. *Neuroscience* 140(1):33–43
- Uusisaari MY, Knopfel T (2012) Diversity of neuronal elements and circuitry in the cerebellar nuclei. *Cerebellum* 11(2):420–421
- Manto M, Gruol D, Schmähmann J, Koibuchi N, Rossi F (2012) *Handbook of the cerebellum and cerebellar disorders*. Springer, New York
- Ito M (2011) *The cerebellum: brain for an implicit self*. FT Press, New Jersey
- Ito M (2006) Cerebellar circuitry as a neuronal machine. *Prog Neurobiol* 78(3–5):272–303
- Llinás RR, Walton KD, Lang EJ (2004) Cerebellum. In: Shepherd GM (ed) *The synaptic organization of the brain*, 5th edn. Oxford University Press, New York, pp 271–310
- Czubayko U, Sultan F, Thier P, Schwarz C (2001) Two types of neurons in the rat cerebellar nuclei as distinguished by membrane potentials and intracellular fillings. *J Neurophysiol* 85(5):2017–2029
- Aizenman CD, Huang EJ, Linden DJ (2003) Morphological correlates of intrinsic electrical excitability in neurons of the deep cerebellar nuclei. *J Neurophysiol* 89(4):1738–1747
- Uusisaari M, Obata K, Knopfel T (2007) Morphological and electrophysiological properties of GABAergic and non-GABAergic cells in the deep cerebellar nuclei. *J Neurophysiol* 97(1):901–911
- Paxinos G, Watson C (2007) *The rat brain in stereotaxic coordinates*, 6th edn. Academic Press, San Diego
- Zhang XY, Yu L, Zhuang QX, Peng SY, Zhu JN, Wang JJ (2013) Postsynaptic mechanisms underlying the excitatory action of histamine on medial vestibular nucleus neurons in rats. *Br J Pharmacol* 170(1):156–169
- Friedman AK, Walsh JJ, Juarez B, Ku SM, Chaudhury D, Wang J, Li X, Dietz DM, Pan N, Vialou VF, Neve RL, Yue Z, Han MH (2014) Enhancing depression mechanisms in midbrain dopamine neurons achieves homeostatic resilience. *Science* 344(6181):313–319
- Lazarov N, Rozloznik M, Reindl S, Rey-Ares V, Dutschmann M, Gratzl M (2006) Expression of histamine receptors and effect of histamine in the rat carotid body chemoafferent pathway. *Eur J Neurosci* 24(12):3431–3444
- Zhang CZ, Zhuang QX, He YC, Li GY, Zhu JN, Wang JJ (2014) 5-HT receptor-mediated excitation on cerebellar fastigial nucleus neurons and promotion of motor behaviors in rats. *Pflugers Arch* 466:1259–1271
- Aizenman CD, Linden DJ (1999) Regulation of the rebound depolarization and spontaneous firing patterns of deep nuclear neurons in slices of rat cerebellum. *J Neurophysiol* 82(4):1697–1709
- de Zeeuw CI, Holstege JC, Ruigrok TJ, Voogd J (1989) Ultrastructural study of the GABAergic, cerebellar, and mesodiencephalic innervation of the cat medial accessory olive: anterograde tracing combined with immunocytochemistry. *J Comp Neurol* 284(1):12–35
- Schwarz C, Schmitz Y (1997) Projection from the cerebellar lateral nucleus to precerebellar nuclei in the mossy fiber pathway is glutamatergic: a study combining anterograde tracing with immunogold labeling in the rat. *J Comp Neurol* 381(3):320–334
- Bagnall MW, Zingg B, Sakatos A, Moghadam SH, Zeilhofer HU, du Lac S (2009) Glycinergic projection neurons of the cerebellum. *J Neurosci* 29(32):10104–10110
- Altman J, Bayer SA (1978) Prenatal development of the cerebellar system in the rat. I. Cytogenesis and histogenesis of the deep nuclei and the cortex of the cerebellum. *J Comp Neurol* 179(1):23–48
- Pugh JR, Raman IM (2008) Mechanisms of potentiation of mossy fiber EPSCs in the cerebellar nuclei by coincident synaptic excitation and inhibition. *J Neurosci* 28(42):10549–10560
- Raman IM, Bean BP (1999) Ionic currents underlying spontaneous action potentials in isolated cerebellar Purkinje neurons. *J Neurosci* 19(5):1663–1674
- Haas HL, Konnerth A (1983) Histamine and noradrenaline decrease calcium-activated potassium conductance in hippocampal pyramidal cells. *Nature* 302(5907):432–434
- Sastry BR, Morishita W, Yip S, Shew T (1997) GABA-ergic transmission in deep cerebellar nuclei. *Prog Neurobiol* 53(2):259–271

38. Edgerton JR, Reinhart PH (2003) Distinct contributions of small and large conductance  $\text{Ca}^{2+}$ -activated  $\text{K}^{+}$  channels to rat Purkinje neuron function. *J Physiol* 548(Pt 1):53–69
39. Inoue I, Yanai K, Kitamura D, Taniuchi I, Kobayashi T, Niimura K, Watanabe T, Watanabe T (1996) Impaired locomotor activity and exploratory behavior in mice lacking histamine H1 receptors. *Proc Natl Acad Sci U S A* 93(23):13316–13320
40. Onodera K, Yamatodani A, Watanabe T, Wada H (1994) Neuropharmacology of the histaminergic neuron system in the brain and its relationship with behavioral disorders. *Prog Neurobiol* 42(6): 685–702
41. Toyota H, Dugovic C, Koehl M, Laposky AD, Weber C, Ngo K, Wu Y, Lee DH, Yanai K, Sakurai E, Watanabe T, Liu C, Chen J, Barbier AJ, Turek FW, Fung-Leung WP, Lovenberg TW (2002) Behavioral characterization of mice lacking histamine H(3) receptors. *Mol Pharmacol* 62(2):389–397
42. Husson Z, Rousseau CV, Broll I, Zeilhofer HU, Dieudonne S (2014) Differential GABAergic and glycinergic inputs of inhibitory interneurons and Purkinje cells to principal cells of the cerebellar nuclei. *J Neurosci* 34(28):9418–9431
43. Pape HC (1996) Queer current and pacemaker: the hyperpolarization-activated cation current in neurons. *Annu Rev Physiol* 58:299–327
44. Uusisaari M, Knopfel T (2010) GlyT2<sup>+</sup> neurons in the lateral cerebellar nucleus. *Cerebellum* 9(1):42–55
45. Li B, Zhu JN, Wang JJ (2014) Histaminergic afferent system in the cerebellum: structure and function. *Cerebellum Ataxias* 1:5
46. Korotkova TM, Haas HL, Brown RE (2002) Histamine excites GABAergic cells in the rat substantia nigra and ventral tegmental area in vitro. *Neurosci Lett* 320(3):133–136
47. Munakata M, Akaike N (1994) Regulation of  $\text{K}^{+}$  conductance by histamine H1 and H2 receptors in neurones dissociated from rat neostriatum. *J Physiol* 480(Pt 2):233–245